



Multifunctional Material Composed of Cesium Salt of Keggin-Type Heteropolytungstate and PtRh/Vulcan Nanoparticles for Electrochemical Oxidation of 2-Propanol in Acidic Medium

Barbara Zakrzewska¹ · Katarzyna Jakubów-Piotrowska¹ · Barbara Gralec¹ · Barbara Kowalewska¹ · Krzysztof Miecznikowski¹

Published online: 29 May 2020

© The Author(s) 2020

Abstract

Platinum–rhodium nanoparticles modified with cesium salt of phosphotungstic acid, CsPTA, have been tested for electro-oxidation of 2-propanol in acidic medium. The resulting Pt-based nanoparticle-containing materials have been carried out using X-ray diffraction (XRD), microscopy (TEM), X-ray photoelectron spectroscopy (XPS), and different electrochemical techniques combining with differential electrochemical mass spectrometry (DEMS). The experimental results such as cyclic voltammetry and chronoamperometry exhibit that films on carbon electrodes composed of CsPTA-modified PtRh/Vulcan nanoparticles improve the catalytic activity, in terms of potential and current densities recorded during electro-oxidation of 2-propanol, relative to the CsPTA-free PtRh/Vulcan nanoparticles. Particularly, the boost in the catalytic current densities is observed at low potential value (below 0.25 V vs. RHE). The differential electrochemical mass spectrometry measurements were utilized to recognize the reaction intermediates as well as products created during the electro-oxidation of 2-propanol. The results indicate that contributions from a straightforward oxidation of 2-propanol to CO₂ are small in comparison to acetone yield.

Keywords Direct alcohol fuel cells · Electro-oxidation of 2-propanol · Cesium salts of heteropoly acid · Pt-based nanoparticles · DEMS

Introduction

The tremendous consumption of fossil fuels in the last century contributed to increased pollution and climate change, which have harmful consequences to us as humans and our planet. Fuel cells are one of the optional technologies to be able to generate eco-friendly energy due to chemical energy is transformed into electrical energy with almost no polluting emissions. Fuel alternatives to hydrogen are various kinds of small organic compounds such as alcohols, organic acids, and esters. Among diverse alcohols, especially methanol, ethanol, ethylene glycol, and 2-propanol are taken into account to be utilized as fuels because their low molecular weights mean that they are easy to transport, store, and handle [1] as well as are already in the liquid state. Furthermore, they possess relatively high theoretical volumetric and gravimetric energy

densities, and better energy efficiencies, contrary to hydrocarbon and gasoline. Among the aforementioned alcohols, ethanol and 2-propanol have higher values of gravimetric energy densities 8.0 and 8.6 kW h kg⁻¹, respectively, and are comparable to hydrocarbons and gasoline (10–11 kW h kg⁻¹). Furthermore, 2-propanol consists of three carbon atoms and one hydroxyl group (–OH) bonding to the middle carbon atom exhibiting a lower permeability through exchange membranes than other alcohols (i.e., methanol and ethanol) resulting in a lower crossover current [2, 3]. Besides, the electro-oxidation of 2-propanol generates a higher number of electrons (18 e⁻) than ethanol (12 e⁻) and 2-propanol is less toxic than methanol. Moreover, electro-oxidation of 2-propanol in contrast to the primary alcohols does not yield CO as an intermediate product due to the bond of the –OH group to the middle carbon atom in 2-propanol leading to difficulties in carbon bond cleavage. In consequence, it has decreased the oxidation onset potential to lower value than, for example, in ethanol and methanol. The anodic oxidation of alcohols consisting of more than two carbon atoms has been investigated relatively less intensively in acidic media than in alkaline ones due to kinetic hindrance and the need for high overpotentials [4–9].

✉ Krzysztof Miecznikowski
kmiecz@chem.uw.edu.pl

¹ Faculty of Chemistry, University of Warsaw, Pasteura 1, 02-093 Warsaw, Poland

Moreover, one drawback of the alkaline medium, for a long electro-oxidation 2-propanol time, is that it is less stable owing to the existence of carbonation effect.

To date, pure platinum (Pt) or Pt alloys have been commonly accepted as a highly efficient catalytic systems toward oxidation of small organic liquid fuel at low temperature energy conversion [10–28], but adsorption of the oxidation products mostly CO-type intermediate causes poisoning of the catalyst surface requiring rather large overpotentials for their withdrawal. At present, few papers have demonstrated the electro-oxidation of 2-propanol when using Pt nanoparticles or Pt alloys in acidic medium [29–32]. In accordance with these studies, it was observed that 2-propanol oxidizes mainly to acetone, as well as small amounts of CO₂, but no CO was detected in contrast to the primary alcohols' oxidation (e.g., ethanol), using Fourier-transform infrared spectroscopy (FTIR) and differential electrochemical mass spectroscopy (DEMS) [4–6, 29–31]. It is generally assumed that the electro-oxidation of 2-propanol produces acetone as a major product and CO₂ due to the preferred 2-propanol dehydrogenation process and rather relative sluggish reaction rate of intermediate species [30, 31]. The presence of acetone is not an advantage, as it may seem, because it also inhibits the surface of platinum catalysts by strong adsorption in both acidic and alkaline media [30, 33, 34]. Recent studies, on the one hand, have shown that systems composed of Rh facilitates the C–C bond breaking, e.g., during electro-oxidation of ethanol [35–40], while Rh itself does not display any activity for electro-oxidation of small organic molecules. On the other hand, there have been reports on the lack of useful role of rhodium-containing systems toward C–C bond breaking. Nart et al. investigated the electro-oxidation of 2-propanol on the platinum–rhodium catalyst in acidic media using the electro-deposition of Pt and Rh on gold substrate [30, 41]. The outcomes showed better electrocatalytic activity toward electro-oxidation of 2-propanol for bimetallic platinum–rhodium electrodes but also increased efficiency for CO₂ formation along with the increase of rhodium content in catalysts. They concluded that the observed effect is rather related to the limited production of the acetone due to the presence of rhodium than enhanced formation of CO₂. In this context, however, the precise role of Rh and how it affects toward C–C bond breaking is complicated and still under strong debate at the elementary level.

More recently, a new approach to attain better electrocatalyst with boosted dissemination of platinum-based nanoparticles has been reported, where the deliberate modification of their surface by adsorption of polyoxometallates toward the development of catalysts for electro-oxidation of small organic compounds was employed [28, 42–45]. Polyoxometallates have several properties that are mutual with transition metal oxide clusters, so they can be viewed as their analogues. Interestingly, by converting heteropoly

acids to their salts, the acid–base and redox properties can be changed and adapted to a desired level. In addition, pristine heteropoly acids are often less stable than their salts. This fact makes the salts of heteropolyacids attractive elements of catalytic systems in electrochemical processes [46, 47], including oxidation of small organic molecules [42–44]. Moreover, it is noteworthy that heteropolyacid salts are generally considered as catalytic materials in various organic reactions such as oxidation of alkanes and alkenes [48, 49], oxidation of carbonyl compounds [50], alkylation of olefins [51], isomerization of olefins [52], and oxidative dehydrogenation of alkanes [53–56].

The purpose of this work was to utilize a catalyst for the 2-propanol electro-oxidation in an acidic media, composed of cesium salt of the Keggin-type heteropolyacid of tungsten (CsPTA) and commercial Vulcan-supported PtRh to enhance activity of electrocatalyst. DEMS measurement was employed to identify the formation of various products (e.g., intermediates) over the electro-oxidation of 2-propanol on CsPTA-modified PtRh/Vulcan nanoparticles and to elucidate the mechanism of the electro-oxidation of 2-propanol under such conditions.

Experimental

All chemical reagents used, if not otherwise mentioned, were high purity and utilized without further purification. Phosphotungstic acid, H₃PW₁₂O₄₀ (PTA), cesium nitrate (CsNO₃), sulfuric acid (99.999%), and 2-propanol (> 99.9%) as well as Nafion and 5% solution of the perfluorinated resin were purchased from Sigma Aldrich. Commercially available 20% PtRh/Vulcan XC-72 nanoparticles (Premetek) were used as catalyst. All electrolytes used were prepared by using twice-distilled water which was finally purified on a Millipore Milli-Q system. Salts of Keggin-type heteropolyacid-modified PtRh/Vulcan nanoparticles were prepared according to the following recipe described in our previous publication [57].

The ratio of platinum to cesium salt of heteropolyacid in examined system was evaluated utilizing X-ray fluorescence (XRF); the resulting ratio was found to be 1:1.2. A catalyst layer on a glassy carbon substrate that was examined for its catalytic activity was formed by dropping a suitable amount of nanoparticle suspension using a pipette and allowing it to dry at ambient conditions. Prior to depositing the catalyst layer on the electrode substrate, the suspensions were sonicated for at least 10 min in order to make uniform solutions. Afterwards, the prepared electrodes with dried layers were modified by dropping on the surface of catalytic layers a 2- μ l aliquot of Nafion (0.02% alcoholic solution) and permitting it to evaporate at room temperature. Finally, the loading of platinum-based catalyst was approximately 100 μ g cm⁻². Before

electro-oxidation experiments were carried out, all catalytic layers were subjected to complete oxidation/reduction cycles in the potential range from 0.0 to 0.8 V in 0.5 mol dm⁻³ H₂SO₄ at a scan rate of 50 mV s⁻¹ until steady-state voltammetric responses were reached.

The electrochemical measurements were carried out in a three-electrode arrangement employing an Hg/Hg₂SO₄ saturated K₂SO₄ reference electrode, a carbon rod as counter electrode, a glassy carbon with a surface area of 0.071 cm² as a working electrode, and using a CH Instruments 750A workstation. All potentials in the present work were expressed versus the reversible hydrogen electrode (RHE). Furthermore, all presented current densities herein were obtained in relation to the geometric surface area of the working electrode. All measurements were carried out in a thermostated cell at temperature of 22 ± 1 °C.

To examine the products' electro-oxidation of 2-propanol in real time, DEMS measurements were performed equipping with a special electrochemical cell coupled to a mass spectrometer. The measurement cell was made based on those proposed by Dube and Brisard [58]. The determination of results of electro-oxidation of 2-propanol during DEMS measurements needs the formation of the layer of catalyst onto a semipermeable membrane with gold electrical contact acting as an interface between two phases (liquid and gas), allowing for the identification of electrode reaction products utilizing MS. The DEMS measurements were performed using an Ivium Stat potentiostat by Ivium Technologies connected with OmniStar gas analysis system, equipped with PrismaPlus QMA 200 M (0–100 amu version) mass spectrometer (MS) from Pfeiffer Vacuum GmbH. To control the MS, Quadera version 4.60 was utilized.

X-Ray photoelectron spectroscopy (XPS) experiments were recorded on a Microlab 350 spectrometer while utilizing Al K α non-monochromatic radiation (1486.6 eV, 300 W) as X-ray excitation. The obtained binding energies have been referred to carbon signal with binding energy equal to 284.2 eV as the internal standard. Each XPS spectrum was fitted to mix Gaussian–Lorentzian line shapes after background subtraction according to Shirley.

Physicochemical features of the used catalytic materials were systematically examined to receive additional information on their crystal structure, composition, and surface morphology by diverse techniques such as transmission electron microscopy (TEM), scanning electron microscopy (SEM), energy dispersion spectroscopy (EDS), and X-ray diffraction (XRD). The TEM investigations were carried out using an equipment operating at 200 keV. Samples for TEM investigations were formed by dropping a diluted suspension of catalytic nanoparticles onto 400-mesh copper grids that supported a Fromvar film (Agar Scientific) and then letting them dry in ambient laboratory conditions. Determination of the crystallographic structure and phase analysis of the investigated

catalysts were performed by XRD using a Bruker D8 Discover system operated with a Cu K α 1 source (λ = 1.5406 Å) and a Vantec (linear) detector (k = 1.5406 Å). The XRD patterns were recorded between diffraction angles of 10° to 100° with a step size of 0.02° s⁻¹. The full width at half-maximum (FWHM) of the proper peak (220) were utilized to find out the average particle size and lattice parameter for each catalyst by the Scherer equation.

Results and Discussion

Figure 1 exhibits the TEM micrographs and corresponding distributions of sizes of the unmodified (a) and modified (b) PtRh/Vulcan nanoparticles. It was clearly displayed that the distribution of fine Pt-based nanoparticles is homogeneous on the surface of supporting material, and the overall nanoparticle sizes are in a narrow range distribution. The average size of pristine PtRh/Vulcan nanoparticles lies in a range of 4–12 nm, with a mean dimension of 8 nm. The average diameter of

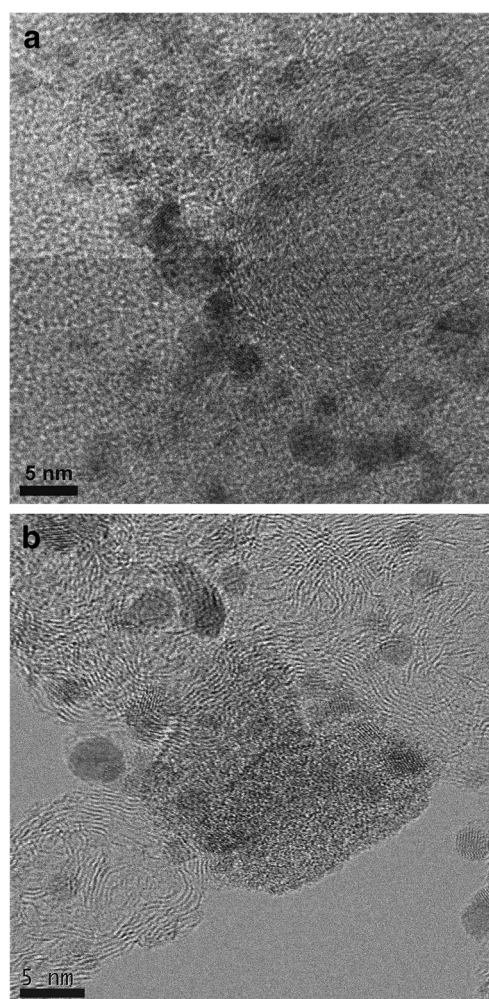


Fig. 1 Transmission electron micrographs (TEMs) of (a) PtRh/Vulcan nanoparticles, (b) CsPTA-modified PtRh/Vulcan

CsPTA-modified PtRh/Vulcan nanoparticles was comparable; they located in the scope of size 7 and 15 nm. The data of Fig. 1 indicates the presence of cesium-substituted phosphotungstic acid (dark gray structures of sizes of 30–50 nm). The cesium salt of phosphotungstic acid structures seems to be joined directly to carbon support materials. Both modified and unmodified PtRh allow nanoparticles that have a quasi-spherical or round shape.

The X-ray diffraction profile of PtRh/Vulcan modified by CsPTA is shown in Fig. 2. The XRD patterns of CsPTA-modified Pt-based catalyst nanoparticles exhibited reflection at 2θ values of around 25° , which corresponded to the facet (002) characteristic of face hexagonal carbon support material [57, 59]. The reflections appeared at about $2\theta = 39.3^\circ$, 45.3° , 66.7° , and 79.9° , and they should be attributed to the (111), (200), (220), and (311) crystalline planes of Pt, respectively. The recorded reflections, in comparison to the literature data for bare Pt (JCPDS no. 04-0802), are slightly shifted to lower 2θ values indicating the influence of alloying [60, 61]. Furthermore, the diffraction peaks that originated from rhodium are not observed directly because their position overlaps with those from platinum [36, 62]. The X-ray diffraction pattern of CsPTA-modified PtRh/Vulcan nanoparticles reveals the additional diffraction peaks at $2\theta = 10.6^\circ$, 18.4° , 23.8° , 26.1° , 30.3° , 35.6° , and 38.9° , which are assigned to the cubic state of cesium-substituted phosphotungstic acid [57]. Moreover, the lattice parameter of the modified PtRh/Vulcan nanoparticles was found to be about 0.3789 nm. The latter value of lattice parameter displacement of PtRh nanoparticles resulting from the presence of cesium salt phosphotungstic acid implies that there is no incorporation of metals (Cs and W) into the Pt lattice that occurred. The average crystallite size of the catalytic materials was calculated from the analysis of Pt (220) peak width analysis utilizing Scherrer's equation. The average

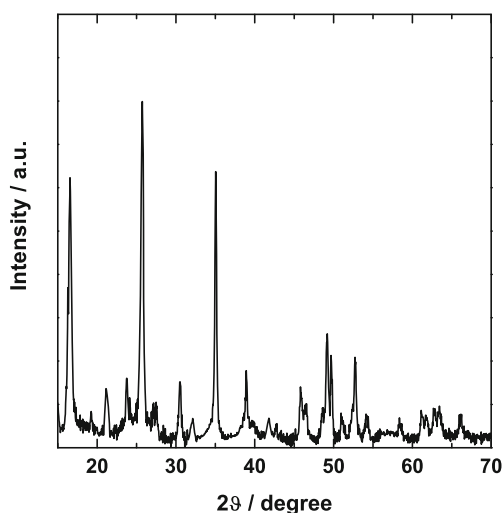


Fig. 2 X-Ray diffraction patterns for the CsPTA-modified PtRh/Vulcan electrocatalyst

PtRh particle size obtained from XRD patterns for modified catalyst was in narrow ranges of 6–11 nm and correlated well with the data presented in our previous work [57]. This outcome is consistent with TEM measurements.

The composition of the surface region as well as the bonding state of PtRh/Vulcan and CsPTA-modified PtRh/Vulcan catalysts was verified using ex situ XPS analysis. As expected, survey scan spectra for CsPTA-modified PtRh/Vulcan clearly confirm the presence of assembled CsPTA on PtRh/Vulcan as recognized by the detection of tungsten (W4f 36 eV) and cesium (Cs3d 725 eV) signals (Fig. 3). The Pt4f region of the spectrum for CsPTA-modified PtRh/Vulcan and pristine PtRh/Vulcan nanoparticles are displayed in Fig. 3A. The deconvolution of Pt 4f peaks were done by using three doublets thus indicating the existence of different Pt chemical state in all cases. In accordance with the literature [40, 63–65], the Pt 4f peak components occurring at binding energies 71.3, 72.0, and 73.9 eV are assigned to the metallic form of Pt as well as various platinum oxides Pt(II) and Pt(IV). Unfortunately, due to the interference of Pt 4d and Rh 3d regions, the Rh 3d spectra, displayed in Fig. 3B, were fitted in the deconvolution doublets for determining Rh amount. Comparing the Rh 3d emission lines for modified and unmodified PtRh/Vulcan nanoparticles, it can be noted that a positive shift is observed. The corresponding XPS spectra of W 4f are also displayed in Fig. 3C and reveal characteristic binding energies of tungsten at 35.8 eV ($4f_{7/2}$ element) and 33.5 eV ($4f_{5/2}$ element), which is consistent with that in pristine cesium salt of heteropolyacid.

To evaluate the catalytic behavior of the test electrode toward the electro-oxidation of 2-propanol, we have performed the cyclic voltammetry measurements over the range 0.0–0.9 V (at 10 mV s^{-1}) and in argon-saturated 0.5 mol dm^{-3} H_2SO_4 . The electrocatalytic materials composed of modified PtRu/Vulcan nanoparticles and bare PtRu/vulcan nanoparticles lodged on a glassy carbon electrode substrate were examined (Fig. 4). It is noteworthy that the cyclic current–potential curves obtained in the supporting electrolyte of the studied catalysts were essentially different in both shape and recorded current density due to the presence of cesium-substituted phosphotungstic acid. The voltammetric measurements on bare PtRh/Vulcan nanoparticles on the electrode surface display two sets of peaks in the hydrogen adsorption–desorption region in the potential lower than 0.3 V because of the oxidation and reduction of hydrogen attached to the alloy surface. At potential between 0.3 and 0.7 V, only capacitive charging is recorded. Furthermore, the appearance of current increase at potential above 0.7 V reflects the generation (at PtRh) of platinum oxides at the platinum alloy surface being typical behavior of systems containing Pt [29, 30]. Repeating the same voltammetric measurements with CsPTA-modified PtRh/Vulcan nanoparticles (red line) results in one peak in the

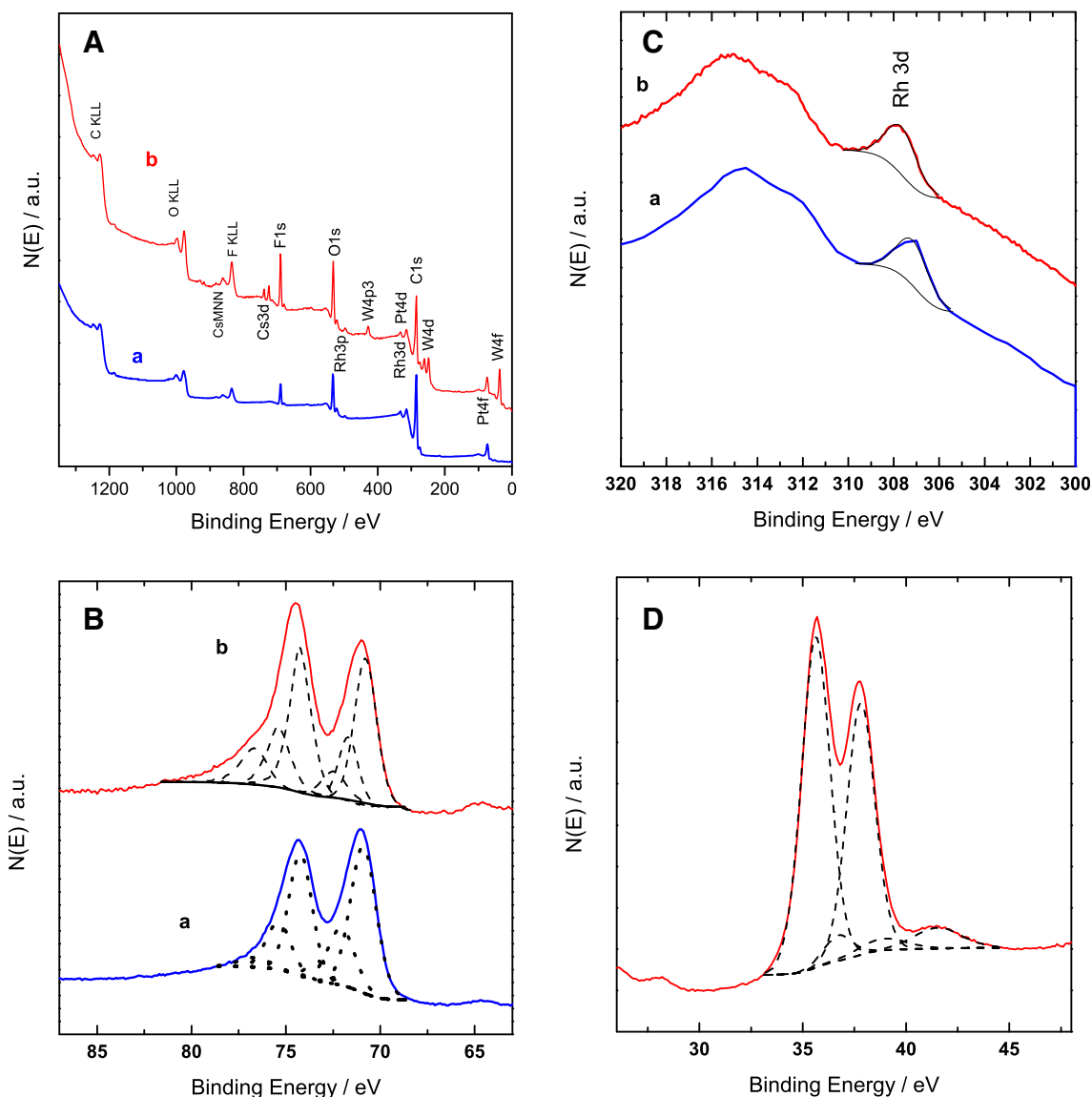


Fig. 3 **A** XPS survey scan for (a) pristine PtRh/Vulcan and (b) CsPTA-modified PtRh/Vulcan. **B** XPS spectra of Pt 4f region recorded for (a) bare Vulcan-supported Pt–Rh nanoparticles and (b) CsPTA-modified

PtRh/Vulcan. **C** XPS spectra recorded in the Rh 3d region for (a) bare PtRh/Vulcan and (b) PtRh/Vulcan modified with CsPTA. **D** XP spectra of the W 4f recorded for the CsPTA-modified PtRh/Vulcan

hydrogen region. This outcome is a consequence of the overlap of the signal originated from the reduction process of CsPTA with hydrogen region on Pt-based catalysts.

To comment on the electrochemical stability of these catalytic materials considered here, the quick tests based on repetitive cyclic voltammetry in the range from 0.0 to 0.9 V in argon-saturated $0.5 \text{ mol dm}^{-3} \text{ H}_2\text{SO}_4$ electrolyte for a period of 2.5 h ($\nu = 50 \text{ mV s}^{-1}$, not shown here) were executed. Repeating the electrochemical stability test for unmodified PtRh/Vulcan nanoparticles was also performed as a reference. It is notable that, with catalytic layer containing CsPTA-modified PtRh/Vulcan, the recorded catalytic current density decreased by about 7% after 250 cycles relative to the initial value. When the aforementioned experimental conditions utilized the pristine PtRh/Vulcan nanoparticles, the respective

decrease was 13%. It therefore seems reasonable to conclude that the presence of CsPTA on the surface of catalyst leads to some improvement in the stability of the anodic current density response, but the more meaningful result of this modification of Pt-based nanoparticles is higher recorded current density for 2-propanol electro-oxidation.

The electrocatalytic activities of the outcome catalysts were investigated during the oxidation of 2-propanol by using cyclic voltammetry. The voltammetric responses in argon-saturated $0.5 \text{ mol dm}^{-3} \text{ H}_2\text{SO}_4$ electrolyte containing 2-propanol at 0.5 mol dm^{-3} concentration of these modified and unmodified PtRh/Vulcan nanoparticles are displayed in Fig. 5. The typical shape of curves show two peaks consistent with the oxidation processes in both anodic and cathodic scans in the considered potential range. The recorded current density

of electro-oxidation of 2-propanol for CsPTA-modified PtRh/Vulcan catalysts starts to rise at potential around 0.12 V reaching the two sets of peak at potential around 0.47 and 0.78 V, which appeared at lower potential observed for unmodified PtRu/Vulcan nanoparticles. The observed electrocatalytic current density (measured at potential above 0.65 V) has a tendency to decrease due to formation of catalytically inactive Pt oxides. In the backward scans, at potentials below 0.70 V, where platinum face is not coated with platinum oxide and becomes once more available for oxidation of 2-propanol or intermediate species, a positive electrocatalytic current is recorded. An important issue also is that lower onset potential of 2-propanol oxidation has been reported following modification of PtRh/Vulcan nanoparticles by CsPTA. By comparing the anodic current densities of alcohol oxidation in cyclic voltammetry measurements in the presence and absence of 2-propanol, the onset potentials of the electro-oxidation of 2-propanol were found. The received values for bare and modified PtRh/Vulcan nanoparticles were 0.20 and 0.12 V, respectively. The outcome implies that the presence of CsPTA leads to a shift in the onset potential toward a more negative value for 2-propanol oxidation of ca. 80 mV. This enhancement effect as well as the higher catalytic current may be caused by a change in surface structure but also the modification of intrinsic electronic structure is not excluded [45]. Furthermore, the obtained lower onset potential in cyclic voltammetric measurements of 2-propanol oxidation with CsPTA-modified PtRh/Vulcan nanoparticles on the electrode substrate is ascribed to rapid dehydrogenation. It was determined that bare Pt or Pt alloy nanoparticles supported on WO_3 or phosphotungstic acid promote a dehydrogenation process

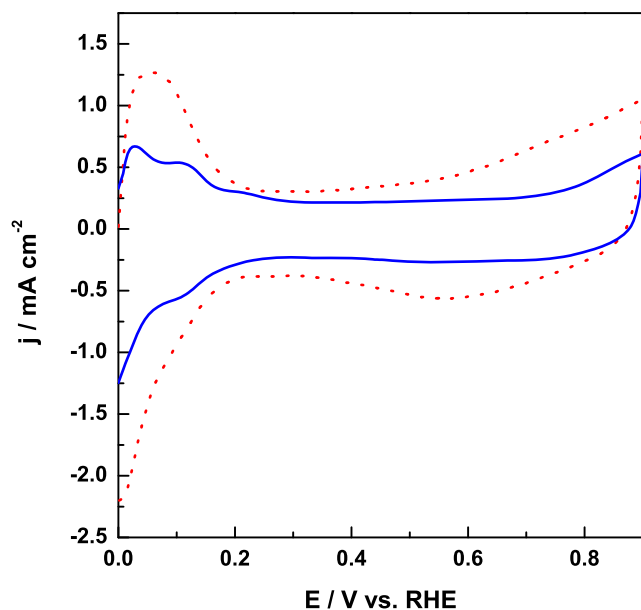


Fig. 4 Cyclic voltammetric responses of PtRh/Vulcan (blue curve) and CsPTA-modified PtRh/Vulcan (red curve). Electrolyte: $0.5 \text{ mol dm}^{-3} \text{ H}_2\text{SO}_4$. Scan rate: 10 mV s^{-1}

[66, 67]. The factors, mentioned previously, referred to modification of Pt-based nanoparticles by CsPTA led to improved mobility of proton and thus easier access to the proton on the electrode surface, providing with a lower onset potential and a higher current density for oxidation of 2-propanol in acidic medium.

To gain some insight into catalytic performance of these materials as electrochemical oxidation catalysts, additional diagnostic experiments were carried out under chronoamperometric conditions during longer periods of time. The test system was 0.5 mol dm^{-3} 2-propanol in $0.5 \text{ mol dm}^{-3} \text{ H}_2\text{SO}_4$ upon employment of fairly low potentials, 0.2 and 0.3 V, in unstirred solution, and the corresponding curves are shown in Fig. 6. The first value of potential was chosen as a value adjacent to the onset potential for 2-propanol electro-oxidation based on the voltammetry experiments, while 0.3 V is matched for potential utilization in fuel cells. The outcomes shown in Fig. 6 confirmed those of the voltammetry measurements in 2-propanol electro-oxidation. It is apparent from Fig. 6 that the initial current density exhibits a rapid decrease with the first period of time followed by an almost constant value for a long time. At both potentials, the highest current density during chronoamperometric measurements were obtained for the catalytic system utilizing PtRh/Vulcan nanoparticles admixed with CsPTA. The reason for this behavior can be related to the presence of cesium-substituted phosphotungstic acid on the surface that is able to either prevent this adsorption or favor the creation of electro-oxidation products that have a minor tendency to link to the active catalytic centers.

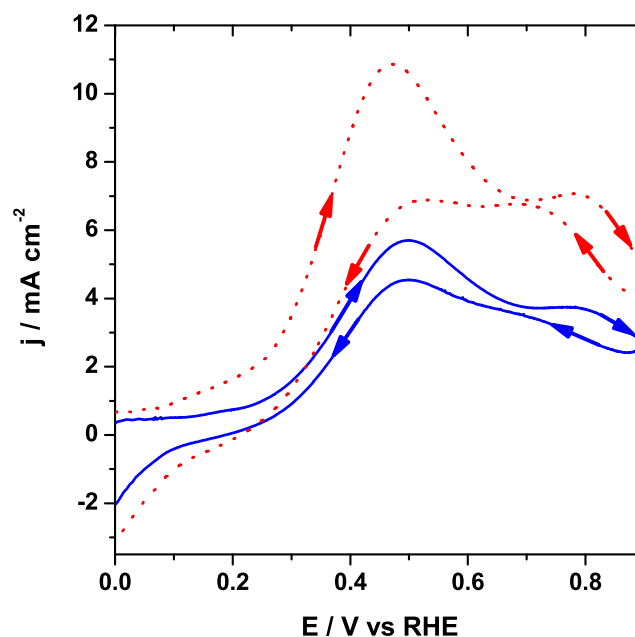


Fig. 5 Cyclic voltammetric responses for oxidation of 0.5 mol dm^{-3} 2-propanol at PtRh/Vulcan (blue curve) and CsPTA-modified PtRh/Vulcan (red curve). Electrolyte: $0.5 \text{ mol dm}^{-3} \text{ H}_2\text{SO}_4$. Scan rate: 5 mV s^{-1} . Arrows indicate the course of potential scan

To identify the formation of products during the 2-propanol electro-oxidation, DEMS, in parallel with electrochemical measurements, was utilized for modified and pristine PtRh/Vulcan nanoparticles. To avoid the eventual changes in the composition or structure alloys, the anodic potential was restricted to 0.9 V throughout the DEMS and electrochemical measurements [68]. The literature overview indicates that the major products of 2-propanol electro-oxidation on Pt are not CO_2 but rather acetone [4–6, 29–31]. Having in mind this fact, for all the catalysts, we examined a few possible products and found only the mass signals $m/z = 58$ for detection of acetone as well as CO_2 $m/z = 44$ and no additional signals were

identified above the detection limit. Both mass signals, $m/z = 58$ and $m/z = 44$, received during voltammetric experiments are presented in Fig. 7 and they display a clear hysteresis between forward and backward scan, which can be linked to the different oxidation states of the catalyst. The $m/z = 58$ ion currents, related to the possible acetone creation, have appeared in the anodic forward scan at potential ca. 0.3 and 0.4 V for modified and unmodified PtRh nanoparticles, respectively (Fig. 7b). It is apparent, upon comparison of typical cyclic voltammetric responses and the ionic currents for bare PtRh/Vulcan nanoparticles and CsPTA-modified PtRh/Vulcan nanoparticles, that the current, obtained at higher potential value (at 0.5 V), was lower for the unmodified sample

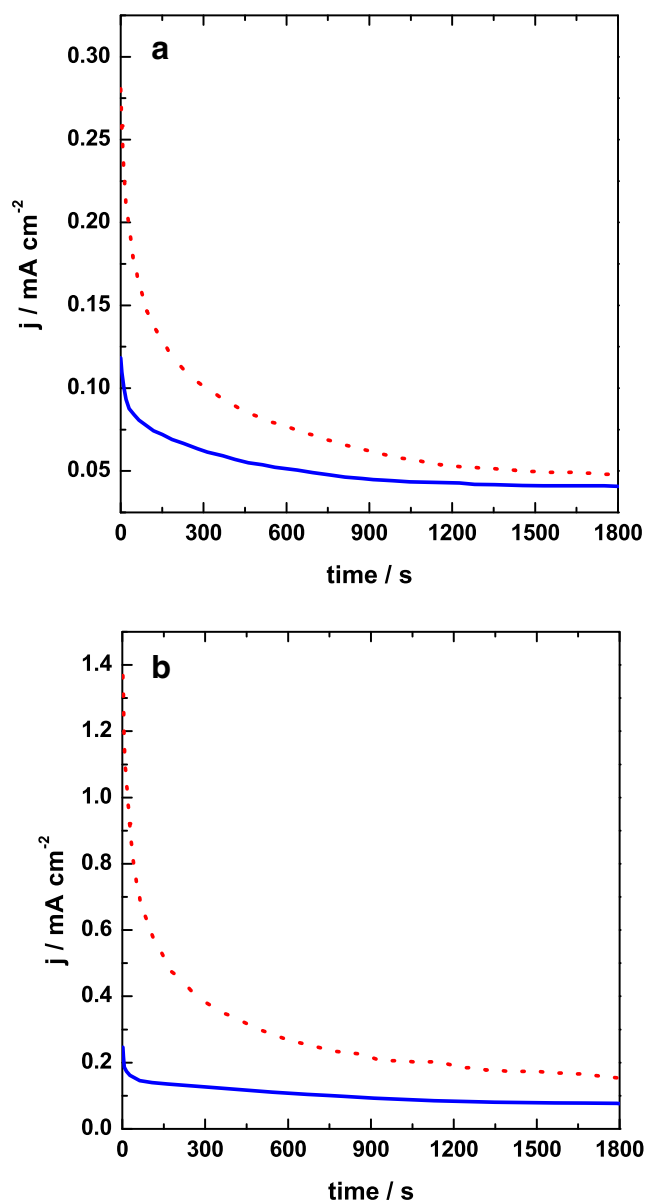


Fig. 6 Current–time responses at 0.2 V (a) and 0.3 V (b) for the oxidation of 0.5 mol dm^{-3} 2-propanol at PtRh/Vulcan (blue curve) and CsPTA-modified PtRh/Vulcan (red curve). Electrolyte: argon saturated $0.5 \text{ mol dm}^{-3} \text{ H}_2\text{SO}_4$

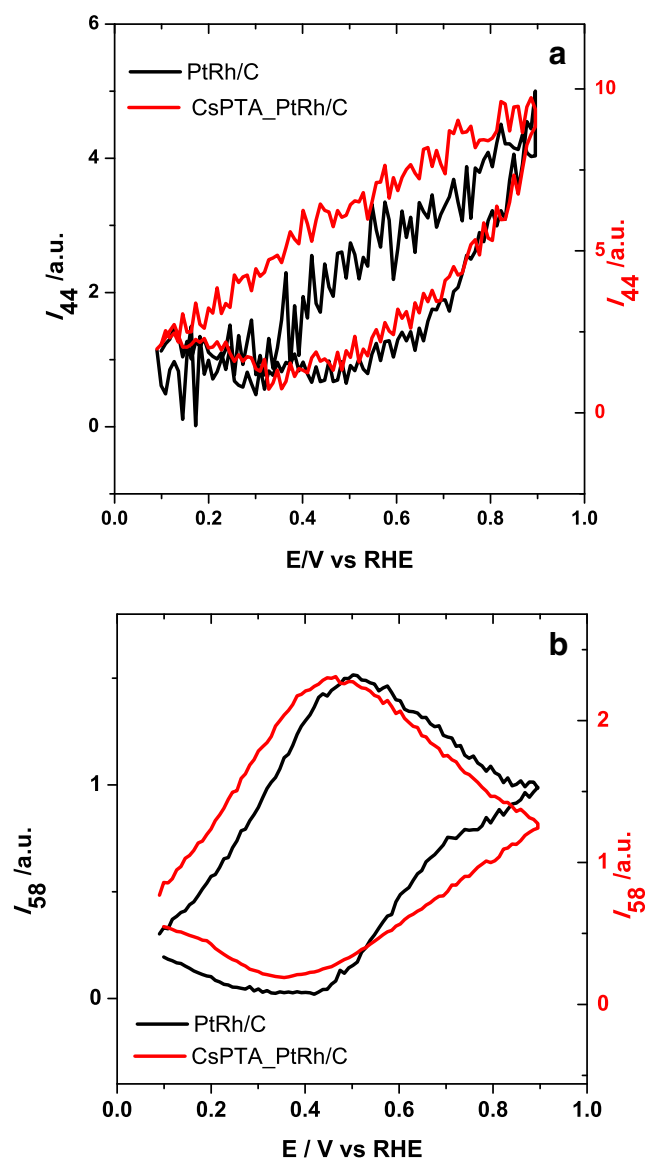


Fig. 7 MFCV outcomes for (a) $m/z = 44$ (CO_2) and (b) $m/z = 58$ (acetone) recorded for pristine PtRh/Vulcan (black curve) and CsPTA-modified PtRh/Vulcan (red curve) nanoparticles. Suitable CV is shown in Fig. 5. Electrolyte: $0.5 \text{ mol dm}^{-3} \text{ H}_2\text{SO}_4 + 0.5 \text{ mol dm}^{-3}$ 2-propanol. Scan rate: 5 mV s^{-1}

in both experiments. Similarly, the $m/z = 44$ ion current signals, associated with the generation of carbon dioxide, are presented in Fig. 7a. The observed mass signal intensity ($m/z = 44$) occurs around 0.4 V in the anodic forward scan, and this signal rises up to 0.9 V. In the reverse direction, CO₂ is generated at potential above 0.5 V, with a peak at 0.5 V. On the basis of the aforementioned outcomes, we can suppose that, in case of cesium salts of phosphotungstic acid–modified sample, the most essential step is the dehydrogenation of adsorbed 2-propanol to form acetone that can further be oxidized to CO₂ with external oxygen from the water [6]. Moreover, these data certainly do not allow us to claim that the rhodium-containing systems facilitate the C–C bond breaking. Hence, the modification of PtRh nanoparticles by CsPTA made some enhancement effect, namely the increase of 2-propanol oxidation current is almost perhaps due to higher acetone production.

Conclusions

The oxidation of 2-propanol in acid medium (0.5 mol dm⁻³ H₂SO₄) was studied at surface of glassy carbon electrode with CsPTA-modified PtRh/Vulcan nanoparticles. The outcomes of the electrochemical diagnostic experiments exhibited that the electrocatalytic activity of PtRh/Vulcan increased in the presence of CsPTA in that lower onset potentials and higher current densities in comparison to pristine Pt-based nanoparticles were noted. The usefulness of the CsPTA is probably related to the improved mobility of proton and availability at the surface of catalysts. The observed improvement in electrocatalytic current under chronoamperometric condition proved the result of the cyclic voltammetric experiments. The catalytic currents for modified and unmodified PtRh/Vulcan nanoparticles have been correlated with the 2-propanol oxidation main product yield. During the 2-propanol electrochemical oxidation at the proposed samples, acetone can be identified as the main product that begins at a rather low potential, and CO₂ is detected as well. The incorporation of cesium-substituted phosphotungstic acid on the surface is able to either prevent this adsorption or favor the creation of electro-oxidation products that have an insignificant tendency to link to the active catalytic centers.

Acknowledgments This work was supported by the National Science Centre (Poland) under project no. 2015/19/B/ST4/03758.

Open Access This article is licensed under a Creative Commons Attribution 4.0 International License, which permits use, sharing, adaptation, distribution and reproduction in any medium or format, as long as you give appropriate credit to the original author(s) and the source, provide a link to the Creative Commons licence, and indicate if changes were made. The images or other third party material in this article are included in the article's Creative Commons licence, unless indicated otherwise in a

credit line to the material. If material is not included in the article's Creative Commons licence and your intended use is not permitted by statutory regulation or exceeds the permitted use, you will need to obtain permission directly from the copyright holder. To view a copy of this licence, visit <http://creativecommons.org/licenses/by/4.0/>.

References

1. M.Z.F. Kamarudin, S.K. Kamarudin, M.S. Masdar, W.R.W. Daud, Review: Direct ethanol fuel cells. *Int. J. Hydrog. Energy* **38**(22), 9438–9453 (2013)
2. D. Cao, S.H. Bergens, A direct 2-propanol polymer electrolyte fuel cell. *J. Power Sources* **124**(1), 12–17 (2003)
3. Z. Qi, A. Kaufman, Performance of 2-propanol in direct-oxidation fuel cells. *J. Power Sources* **112**(1), 121–129 (2002)
4. S.-G. Sun, Y. Lin, Kinetic aspects of oxidation of isopropanol on Pt electrodes investigated by in situ time-resolved FTIR spectroscopy. *J. Electroanal. Chem.* **375**(1-2), 401–404 (1994)
5. S.-G. Sun, Y. Lin, *Electrochim. Acta* **41**(5), 693–700 (1996)
6. E. Pastor, S. González, A.J. Arvia, Electroreactivity of isopropanol on platinum in acids studied by DEMS and FTIRS. *J. Electroanal. Chem.* **395**(1-2), 233–242 (1995)
7. A. Serov, U. Martinez, A. Falase, P. Atanassov, Highly active PdCu catalysts for electrooxidation of 2-propanol. *Electrochem. Commun.* **22**, 193–196 (2012)
8. M.E.P. Markiewicz, D.M. Hebert, S.H. Bergens, Electro-oxidation of 2-propanol on platinum in alkaline electrolytes. *J. Power Sources* **161**(2), 761–767 (2006)
9. A. Santasalo-Aamio, Y. Kwon, E. Ahlberg, K. Kontturi, T. Kallio, M.T.M. Koper, Comparison of methanol, ethanol and iso-propanol oxidation on Pt and Pd electrodes in alkaline media studied by HPLC. *Electrochem. Commun.* **13**(5), 466–469 (2011)
10. E. Antolini, Carbon supports for low-temperature fuel cell catalysts. *Appl. Catal. B Environ.* **88**(1-2), 1–24 (2009)
11. C. Lamy, A. Lima, V. LeRhun, F. Delime, C. Coutanceau, J.-M. Léger, Recent advances in the development of direct alcohol fuel cells (DAFC). *J. Power Sources* **105**(2), 283–296 (2002)
12. Z. Jusys, T.J. Schmidt, L. Dubau, K. Lasch, L. Jörissen, J. Garche, R.J. Behm, Activity of PtRuMeOx (Me = W, Mo or V) catalysts towards methanol oxidation and their characterization. *J. Power Sources* **105**(2), 297–304 (2002)
13. M. Li, D.A. Cullen, K. Sasaki, N.S. Marinkovic, K. More, R.R. Adzic, Ternary Electrocatalysts for Oxidizing Ethanol to Carbon Dioxide: Making Ir Capable of Splitting C–C Bond. *J. Am. Chem. Soc.* **135**(1), 132–141 (2013)
14. J. Mann, N. Yao, A.B. Bocarsly, Characterization and Analysis of New Catalysts for a Direct Ethanol Fuel Cell†. *Langmuir* **22**(25), 10432–10436 (2006)
15. H. Wang, Z. Jusys, R.J. Behm, Ethanol electro-oxidation on carbon-supported Pt, PtRu and Pt3Sn catalysts: A quantitative DEMS study. *J. Power Sources* **154**(2), 351–359 (2006)
16. F. Colmati, E. Antolini, E.R. Gonzalez, Effect of temperature on the mechanism of ethanol oxidation on carbon supported Pt, PtRu and Pt3Sn electrocatalysts. *J. Power Sources* **157**(1), 98–103 (2006)
17. G. Li, P.G. Pickup, The promoting effect of Pb on carbon supported Pt and Pt/Ru catalysts for electro-oxidation of ethanol. *Electrochim. Acta* **52**(3), 1033–1037 (2006)
18. A.O. Neto, R.R. Dias, M.M. Tusi, M. Linardi, E.V. Spinacé, Electro-oxidation of methanol and ethanol using PtRu/C, PtSn/C and PtSnRu/C electrocatalysts prepared by an alcohol-reduction process. *J. Power Sources* **166**(1), 87–91 (2007)
19. K. Miecznikowski, P.J. Kulesza, Activation of dispersed PtSn/C nanoparticles by tungsten oxide matrix towards more efficient oxidation of ethanol. *J. Power Sources* **196**(5), 2595–2601 (2011)

20. K. Miecznikowski, Enhancement of activity of PtRh nanoparticles towards oxidation of ethanol through modification with molybdenum oxide or tungsten oxide. *J. Solid State Electrochem.* **16**(8), 2723–2731 (2012)
21. J.M. Sieben, M.M.E. Duarte, Methanol, ethanol and ethylene glycol electro-oxidation at Pt and Pt–Ru catalysts electrodeposited over oxidized carbon nanotubes. *Int. J. Hydrog. Energy* **37**(13), 9941–9947 (2012)
22. X. Zhang, Z. Tian, P.K. Shen, Composite of nanosized carbides and carbon aerogel and its supported Pd electrocatalyst for synergistic oxidation of ethylene glycol. *Electrochem. Commun.* **28**, 9–12 (2013)
23. T. Ramulifho, K.I. Ozoemena, R.M. Modibedi, C.J. Jafta, M.K. Mathe, Electrocatalytic oxidation of ethylene glycol at palladium-bimetallic nanocatalysts (PdSn and PdNi) supported on sulfonate-functionalised multi-walled carbon nanotubes. *J. Electroanal. Chem.* **692**, 26–30 (2013)
24. M. Chatterjee, A. Chatterjee, S. Ghosh, I. Basumallick, Electro-oxidation of ethanol and ethylene glycol on carbon-supported nano-Pt and -PtRu catalyst in acid solution. *Electrochim. Acta* **54**(28), 7299–7304 (2009)
25. Q. Liu, Y.-R. Xu, A.-J. Wang, J.-J. Feng, Simple wet-chemical synthesis of core–shell Au–Pd@Pd nanocrystals and their improved electrocatalytic activity for ethylene glycol oxidation reaction. *Int. J. Hydrog. Energy* **41**(4), 2547–2553 (2016)
26. Y. Yang, W. Wang, Y. Liu, F. Wang, Z. Zhang, Z. Lei, Carbon supported heterostructured Pd–Ag nanoparticle: Highly active electrocatalyst for ethylene glycol oxidation. *Int. J. Hydrog. Energy* **40**(5), 2225–2230 (2015)
27. F.E. López-Suárez, C.T. Carvalho-Filho, A. Bueno-López, J. Arboleda, A. Echavarría, K.I.B. Eguiluz, G.R. Salazar-Banda, Platinum–tin/carbon catalysts for ethanol oxidation: Influence of Sn content on the electroactivity and structural characteristics. *Int. J. Hydrog. Energy* **40**(37), 12674–12686 (2015)
28. P.J. Kulesza, I.S. Pieta, I.A. Rutkowska, A. Wadas, D. Marks, K. Klak, L. Stobinski, J.A. Cox, Electrocatalytic oxidation of small organic molecules in acid medium: Enhancement of activity of noble metal nanoparticles and their alloys by supporting or modifying them with metal oxides. *Electrochim. Acta* **110**, 474–483 (2013)
29. S.-G. Sun, D.-F. Yang, Z.-W. Tian, In situ FTIR studies on the adsorption and oxidation of n-propanol and isopropanol at a platinum electrode in sulphuric acid solutions. *J. Electroanal. Chem. Interfacial Electrochem.* **289**(1–2), 177–187 (1990)
30. I.A. Rodrigues, F.C. Nart, 2-Propanol oxidation on platinum and platinum–rhodium electrodeposits. *J. Electroanal. Chem.* **590**(2), 145–151 (2006)
31. R.G.C.S. Reis, C.A. Martins, G.A. Camara, The Electrooxidation of 2-Propanol: An Example of an Alternative Way to Look at In Situ FTIR Data. *Electrocatalysis* **1**(2–3), 116–121 (2010)
32. J.F. Gomes, V.L. Oliveira, P.M.P. Pratta, G. Tremiliosi-Filho, Reactivity of Alcohols with Three-Carbon Atom Chain on Pt in Acidic Medium. *Electrocatalysis* **6**(1), 7–19 (2015)
33. Y. Cheng, Y. Liu, D. Cao, G. Wang, Y. Gao, Effects of acetone on electrooxidation of 2-propanol in alkaline medium on the Pd/Ni-foam electrode. *J. Power Sources* **196**(6), 3124–3128 (2011)
34. Y. Liu, Y. Zeng, R. Liu, H. Wu, G. Wang, D. Cao, Poisoning of acetone to Pt and Au electrodes for electrooxidation of 2-propanol in alkaline medium. *Electrochim. Acta* **76**, 174–178 (2012)
35. A. Kowal, M. Li, M. Shao, K. Sasaki, M.B. Vukmirovic, J. Zhang, N.S. Marinkovic, P. Liu, A.I. Frenkel, R.R. Adzic, Ternary Pt/Rh/SnO₂ electrocatalysts for oxidizing ethanol to CO₂. *Nat. Mater.* **8**(4), 325–330 (2009)
36. M. Li, A. Kowal, K. Sasaki, N. Marinkovic, D. Su, E. Korach, P. Liu, R.R. Adzic, Ethanol oxidation on the ternary Pt–Rh–SnO₂/C electrocatalysts with varied Pt:Rh:Sn ratios. *Electrochim. Acta* **55**(14), 4331–4338 (2010)
37. F.H.B. Lima, D. Profeti, W.H. Lizcano-Valbuena, E.A. Ticianelli, E.R. Gonzalez, Carbon-dispersed Pt–Rh nanoparticles for ethanol electro-oxidation. Effect of the crystallite size and of temperature. *J. Electroanal. Chem.* **617**(2), 121–129 (2008)
38. A.B. Delpuech, T. Asset, M. Chatenet, C. Cremers, Electrooxidation of Ethanol at Room Temperature on Carbon-Supported Pt and Rh-Containing Catalysts: A DEMS Study. *J. Electrochem. Soc.* **161**(9), F918–F924 (2014)
39. A. Bach Delpuech, F. Maillard, M. Chatenet, P. Soudant, C. Cremers, Ethanol oxidation reaction (EOR) investigation on Pt/C, Rh/C, and Pt-based bi- and tri-metallic electrocatalysts: A DEMS and in situ FTIR study. *Appl. Catal. B Environ.* **181**, 672–680 (2016)
40. J. Piwowar, A. Lewera, ChemRxiv. Preprint. (2018) <https://doi.org/10.26434/chemrxiv.6281264.v1>
41. I.A. Rodrigues, K. Bergamaski, F.C. Nart, Probing n-Propanol Electrochemical Oxidation on Bimetallic PtRh Codeposited Electrodes. *J. Electrochem. Soc.* **150**(2), E89 (2003)
42. A. Zurowski, A. Kolary-Zurowska, S. Dsoke, P.J. Barczuk, R. Marassi, P.J. Kulesza, Activation of carbon-supported platinum nanoparticles by zeolite-type cesium salts of polyoxometallates of molybdenum and tungsten towards more efficient electrocatalytic oxidation of methanol and ethanol. *J. Electroanal. Chem.* **649**(1–2), 238–247 (2010)
43. P.J. Barczuk, A. Lewera, K. Miecznikowski, A. Zurowski, P.J. Kulesza, Enhancement of catalytic activity of platinum-based nanoparticles towards electrooxidation of ethanol through interfacial modification with heteropolymolybdates. *J. Power Sources* **195**(9), 2507–2513 (2010)
44. A. Lewera, P.J. Barczuk, K. Skorupska, K. Miecznikowski, M. Salamonczyk, P.J. Kulesza, Influence of polyoxometallate on oxidation state of tin in Pt/Sn nanoparticles and its importance during electrocatalytic oxidation of ethanol – Combined electrochemical and XPS study. *J. Electroanal. Chem.* **662**(1), 93–99 (2011)
45. D.M. Han, Z.P. Guo, R. Zeng, C.J. Kim, Y.Z. Meng, H.K. Liu, Multiwalled carbon nanotube-supported Pt/Sn and Pt/Sn/PMO₁₂ electrocatalysts for methanol electro-oxidation. *Int. J. Hydrog. Energy* **34**(5), 2426–2434 (2009)
46. J.S. Santos, J.A. Dias, S.C.L. Dias, F.A.C. Garcia, J.L. Macedo, F.S.G. Sousa, L.S. Almeida, Mixed salts of cesium and ammonium derivatives of 12-tungstophosphoric acid: Synthesis and structural characterization. *Appl. Catal. A Gen.* **394**(1–2), 138–148 (2011)
47. A. Corma, A. Martinez, C. Martínez, *J. Catal.* **164**(2), 422–432 (1996)
48. P. Shringarpure, K. Patel, A. Patel, First Series Transition Metal Substituted Phosphotungstates as Catalysts for Selective Non-Solvent Liquid Phase Oxidation of Styrene to Benzaldehyde: A Comparative Study. *J. Clust. Sci.* **22**(4), 587–601 (2011)
49. S. Pathan, A. Patel, Transition-Metal-Substituted Phosphomolybdates: Catalytic and Kinetic Study for Liquid-Phase Oxidation of Styrene. *Ind. Eng. Chem. Res.* **52**(34), 11913–11919 (2013)
50. O.A. Kholdeeva, M.N. Timofeeva, G.M. Maksimov, R.I. Maksimovskaya, W.A. Neiwert, C.L. Hill, Aerobic Oxidation of Formaldehyde Mediated by a Ce-Containing Polyoxometalate under Mild Conditions. *Inorg. Chem.* **44**(3), 666–672 (2005)
51. P. Tundo, A. Perosa, F. Zecchini, *Methods and Reagents for Green Chemistry: An Introduction* (John Wiley & Sons, Inc., Hoboken, 2007)
52. B.B. Bardin, R.J. Davis, *Top. Catal.* **6**(1/4), 77–86 (1998)
53. J.-S. Min, N. Mizuno, Effects of additives on catalytic performance of heteropoly compounds for selective oxidation of light alkanes. *Catal. Today* **71**(1–2), 89–96 (2001)

54. M. Sun, J. Zhang, C. Cao, Q. Zhang, Y. Wang, H. Wan, Significant effect of acidity on catalytic behaviors of Cs-substituted polyoxometalates for oxidative dehydrogenation of propane. *Appl. Catal. A Gen.* **349**(1-2), 212–221 (2008)
55. Q. Zhang, C. Cao, T. Xu, M. Sun, J. Zhang, Y. Wang, H. Wan, *Chem. Commun.* 2376–2378 (2009). <https://doi.org/10.1039/B823369A>
56. N. Mizuno, J.-S. Min, A. Taguchi, Preparation and Characterization of Cs_{2.8}H_{1.2}PMo₁₁Fe(H₂O)O₃₉·6H₂O and Investigation of Effects of Iron-Substitution on Heterogeneous Oxidative Dehydrogenation of 2-Propanol. *Chem. Mater.* **16**(14), 2819–2825 (2004)
57. L. Adamczyk, J.A. Cox, K. Miecznikowski, Activation of a Pt-based alloy by a Keggin-type cesium salt of heteropolytungstate towards electrochemical oxidation of ethylene glycol in acidic medium. *Int. J. Hydrog. Energy* **42**(8), 5035–5046 (2017)
58. P. Dubé, G.M. Brisard, Influence of adsorption processes on the CO₂ electroreduction: An electrochemical mass spectrometry study. *J. Electroanal. Chem.* **582**(1-2), 230–240 (2005)
59. J. Wang, G. Yin, Y. Shao, S. Zhang, Z. Wang, Y. Gao, Effect of carbon black support corrosion on the durability of Pt/C catalyst. *J. Power Sources* **171**(2), 331–339 (2007)
60. D.M. dos Anjos, F. Hahn, J.-M. Léger, K.B. Kokoh, G. Tremiliosi-Filho, Ethanol electrooxidation on Pt-Sn and Pt-Sn-W bulk alloys. *J. Braz. Chem. Soc.* **19**(4), 795–802 (2008)
61. S. Tanaka, M. Umeda, H. Ojima, Y. Usui, O. Kimura, I. Uchida, Preparation and evaluation of a multi-component catalyst by using a co-sputtering system for anodic oxidation of ethanol. *J. Power Sources* **152**, 34–39 (2005)
62. F.H.B. Lima, E.R. Gonzalez, Ethanol electro-oxidation on carbon-supported Pt–Ru, Pt–Rh and Pt–Ru–Rh nanoparticles. *Electrochim. Acta* **53**(6), 2963–2971 (2008)
63. J.F. Moulder, W.F. Stickle, P.E. Sobol, K.D. Bomben, *Handbook of X-Ray Photoelectron Spectroscopy: A Reference Book of Standard Spectra for Identification and Interpretation of XPS Data* (Perkin-Elmer Corporation, Eden Prairie, 1992)
64. A. Lewera, W.P. Zhou, C. Vericat, J.H. Chung, R. Haasch, A. Wieckowski, P.S. Bagus, XPS and reactivity study of bimetallic nanoparticles containing Ru and Pt supported on a gold disk. *Electrochim. Acta* **51**(19), 3950–3956 (2006)
65. W.-P. Zhou, A. Lewera, P.S. Bagus, A. Wieckowski, Electrochemical and Electronic Properties of Platinum Deposits on Ru(0001): Combined XPS and Cyclic Voltammetric Study. *J. Phys. Chem. C* **111**(36), 13490–13496 (2007)
66. A.C.C. Tseung, K.Y. Chen, Hydrogen spill-over effect on Pt/WO₃ anode catalysts. *Catal. Today* **38**(4), 439–443 (1997)
67. P.K. Shen, A.C.C. Tseung, Anodic Oxidation of Methanol on Pt/WO₃ in Acidic Media. *J. Electrochem. Soc.* **141**(11), 3082 (1994)
68. M.K. Aston, D.A.J. Rand, R. Woods, Cyclic voltammetric investigation of platinum-rhodium alloys. *J. Electroanal. Chem. Interfacial Electrochem.* **163**(1-2), 199–207 (1984)

Publisher's Note Springer Nature remains neutral with regard to jurisdictional claims in published maps and institutional affiliations.